

Electron-lattice interaction in ionic and partially ionic solids*

R. S. Bauer

Xerox Palo Alto Research Center, Palo Alto, California 94304

S. F. Lin and W. E. Spicer

Stanford Electronics Laboratories, Stanford University, Stanford, California 94305

(Received 15 April 1976)

We examine the interaction of electrons with the lattice in solids where the resulting influence on electronic states is so large ($> 10k_B\Delta T$) that the process cannot properly be explained in terms of phonon scattering. A general description is given of temperature effects on photoemission so that we could properly use this tool to study electron (and vibrational) states. We propose a microscopic description in terms of a dynamic modulation of the orbital hybridization. While transition matrix elements may be effected, proper magnitudes for experimental peak broadening and its temperature dependence are calculated on the basis of density of states modulation alone. This phenomenon can be used to identify the atomic origin of certain photoemission (and optical absorption) peaks, as demonstrated for d states in the noble-metal halides (and KBr). General criteria are established for a solid to exhibit such strong (yet not Frank-Condon) electron-lattice coupling. Generally speaking, the valence states of solids which have an ionicity midway between pure covalent and pure ionic ($0.86 > f_i > 0.73$), and certain conduction states of more ionic materials ($1 > f_i > 0.86$) should exhibit the necessary dynamic hybridization. We also consider effects of this interaction on the vibrational states.

I. INTRODUCTION

The recent work of Phillips and Van Vechten¹ to classify solids according to a scale of ionicities has shown striking changes in many properties of solids with ionicities in the neighborhood of a structural transformation. In the case of A^mB^{8-N} compounds we refer to these as "partially ionic" solids because of their location between ionic alkali-halide-type insulators and purely covalent semiconductors such as silicon. The relative instability of the structure of these solids is caused by the electronic energy states being a complex balance of contributions. The noble-metal halides are a prime example since the relative mixing of the metal d electrons in forming the valence states causes these solids to be either rock-salt (AgBr and AgCl) or zinc-blende (AgI and the copper salts) structure at room temperature.

We have conducted a detailed photoemission investigation of the electronic states of the silver halides in order to study the location and role of the states derived from the atomic Ag ($4d$) orbitals.² In an attempt to sharpen broad structure in the energy-distribution curves (EDC's) of photoemitted electrons, the samples were cooled below the Debye temperature Θ_D . Certain structure was discovered³ to sharpen by over an order of magnitude more than the change in thermal energy $\Delta k_B T$. Extension of this work to other solids like TlCl,⁴ and CuBr,⁵ has supported the original idea that such effects are due to a very strong interaction of the electrons with the lattice. While not large enough to require the Frank-Condon principle, the electron-lattice interaction in these

partially-ionic solids must be understood to interpret their electronic and phonon states properly.

In this paper we examine microscopic aspects of this interaction. Following examination of possible temperature effects on photoemission from solids in Sec. II, we propose a very general description of dynamic wave-function hybridization through which the lattice vibrations affect the electron states. This leads to effects mainly in the density of states, but can also cause transition-matrix-element changes. Using this general picture for the physical phenomenon, one can identify the atomic origin of certain EDC (and associated optical absorption) peaks. In Sec. IV we quantify these considerations by making certain simplifying assumptions about the states involved, the nature of the lattice vibrations and the extent of the electronic interactions. These computations demonstrate the plausibility of dynamic hybridization by predicting the proper magnitudes for experimental peak broadening and its temperature dependence. We then establish in Sec. V some general criteria for a solid to exhibit this type of electron-lattice interaction.⁶ We conclude by considering effects of this electron-lattice coupling on the vibrational states and its possible importance in superconductivity.

II. TEMPERATURE EFFECTS ON PHOTOEMISSION

The effects of lattice vibrations in photoemission are most easily handled by considering the photoemission as a three-step process⁷: optical excitation of an electron followed by transport to the surface of the solid with eventual escape into vacu-

um. In considering the effects of temperature variation on photoemission, it is most helpful to consider the effects in each of these steps separately.

A. Escape

In order for the photoelectron to escape from the solid into vacuum, it must overcome the potential energy barrier at the surface. The energy associated with the velocity component normal to the surface must be greater than the electron affinity. This defines a "cone" of velocities with which an electron can escape the solid. The probability T for an electron with energy E at the surface to escape from the solid can be used to define the escape step.

In practice, $T(E)$ has variously been taken as a step function, a free-electron escape function with an $E^{1/2}$ dependence, used as a phenomenological variable, or has been determined using band theory. This function will be affected by any changes in the surface potential (e.g., change in population of the surface states), by scattering events associated with the escape, or by a change in the electron affinity. The important point to realize for the studies summarized here is that a change in $T(E)$ upon cooling will be seen primarily near threshold and will be uniform for all the EDC's. As seen in Fig. 1, when large EDC changes are observed, they occur many eV above the threshold. Thus, an enhanced photoelectron escape is not the process which is of primary importance. The possibility of an increased escape probability due to enhanced scattering into the escape cone will be considered in Sec. II B on transport.

B. Transport

The photoelectron can change its energy by inelastic scattering on the way to the surface. The scattering processes of importance when considering temperature variations are those which involve the creation (emission) or annihilation (absorption) of a phonon. The resulting changes in the electron energy will appear in the measured EDC as a replica of the actual final state energy just after the optical excitation which is broadened and slightly shifted to lower energies. This will also occur if the interaction with the lattice is viewed as a polaron whereby the electron energy is continually decreased as it moves through the solid by an amount depending on the electron's velocity.⁸ Since the escape depths of the photoelectrons at these energies are normally less than 100 Å when the final-state energies are above the threshold for pair production,⁷ the total scattering history of any electron usually involves only a small

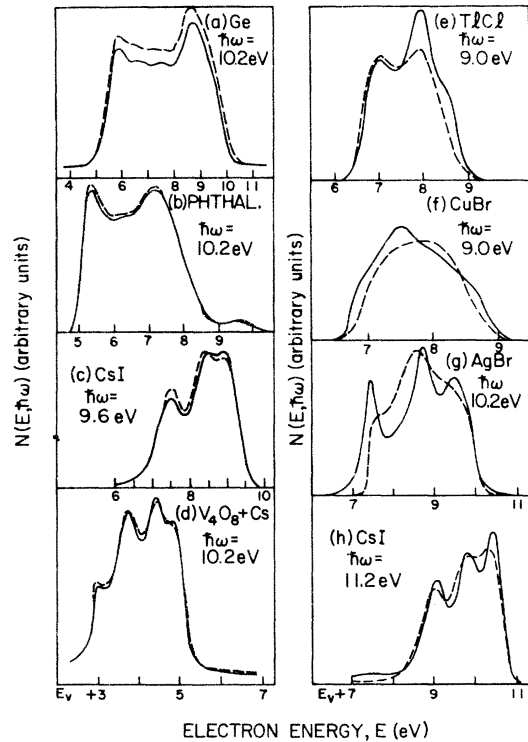


FIG. 1. Comparison of energy distributions for electrons photoemitted from (a) Ge, (b) metal-free phthalocyanine, (c) and (h) CsI, (d) $V_4O_8 + Cs$, (e) TlCl, (f) CuBr, (g) AgBr at 77°K (—) and 295°K (---) for photon energy $\hbar\omega$. Electron energy is referred to the valence-band maximum E_v . Caution should be taken in comparing the heights of curves since they are either chosen arbitrarily for (b), (c), and (h) or normalized to the incident rather than absorbed photon flux for the others. The data are from (a) T. M. Donovan, Ph.D. dissertation (Stanford University, 1970) (unpublished) (Xerox University Microfilms No. 71-12887); (b) B. H. Schechtman, Ph.D. dissertation (Stanford University, 1969) (unpublished) (Xerox University Microfilms No. 69-14014); (c) and (h), T. H. DiStefano, Ph.D. dissertation (Stanford University, 1970) (unpublished) (Xerox University Microfilms No. 71-2755); T. H. DiStefano and W. E. Spicer, Phys. Rev. B **7**, 1554 (1973); (d) G. F. Derbenwick, Ph.D. dissertation (Stanford University, 1970) (unpublished) (Xerox University Microfilms No. 72-12882); (e) Ref. 4; (f) Ref. 5; and (g) Ref. 2. Another good example is LiI by T. H. DiStefano, Ph.D. dissertation (Stanford University, 1970) (unpublished) (Xerox University Microfilms No. 71-2755) and published in Ref. 3.

number of phonons. In the silver halides, the LA phonon energy is on the order of 8 meV and the LO phonon energy around 20 meV.⁹ Thus, the energies involved in such scattering events are normally much less than 0.1 eV. As the temperature is lowered, the probability of absorbing a phonon is greatly diminished and hence the electron-phonon interaction will be reduced. This will

cause a sharpening in EDC structure and a shift to high energies due to the asymmetry of this narrowing. However, since the energies in the high-temperature broadening are so small to begin with, the sharpening and shifting of EDC structure when pair production is possible will be very small, normally being comparable to the change in $k_B T$. The change in the photoemission upon cooling a wide variety of solids are quite small [see Figs. 1(a)–1(d)]. For the most part, these changes can be explained simply by this process of absorption or emission of a few phonons by the photoexcited electron.

The final-state energy of the photoelectron following excitation may be greater than the electron affinity of the solid but, because of the direction of its velocity, it may not fall within the escape cone; if this is the case and if its velocity remains unperturbed, it will not be emitted into vacuum. The electron may, however, interact with the lattice thereby changing its real momentum but not appreciably changing its energy. There is then the possibility of scattering into the escape cone and obtaining an enhanced number of electrons emitted.¹⁰ Such a scattering process would be temperature dependent by virtue of the temperature dependence of the lattice vibration. The major effect this would have on the EDC's is a rather uniform increase of the peak strengths with increasing temperature. However, this would probably only broaden the structure on the order of several optical phonon energies, about 50 meV. This is clearly too small to explain, for example, the measured silver halide temperature-dependent broadening in Fig. 1(g). It is further in the wrong direction to explain most of the variation in peak strengths with temperature.

C. Optical transition

Considering the effect of temperature variation on the excitation, we must examine both the transition and the states involved in the transition separately. The latter will be discussed in Sec. III. The transition matrix elements will mainly serve to suppress or enhance any temperature dependence present in the density of states because it simply "projects out" part of the hybridized basis function. Thus, one expects the matrix elements to mainly affect the observed electronic state temperature dependence in different photon energy ranges,^{11,12} but not to be as strongly material dependent as Fig. 1 demonstrates.

III. ELECTRONIC STATES

Based on the preceding, it is reasonable to expect that what is occurring in the EDC's is char-

acteristic of the electronic states of the solid rather than the photoemission used to study them. A more complete discussion of various mechanisms causing thermal effects is given in Reference 2.

A. Temperature effects

Two important experimental findings must be explained. First, the thermal effect is only observed for a few solids having intermediate bonding. This generally includes valence states of partially ionic solids and conduction states of ionic solids having d character. Secondly, the effect is selective according to the electronic state. This is clearly observed in the series of AgBr EDC's shown in Fig. 2. For example, independent of photon energy, structure is temperature independent for electron energies within 1.5–2.0 eV of the upper edge of the curves and for the peak emerging at $h\nu = 11.0$ eV (i.e., 3.7 eV below this edge). For initial states in the ~ 1.5 eV intermediate region, the thermal modulation is striking.

There are a number of mechanisms for thermal influences on electronic states which cannot explain these two very general results. One natural approach to the problem is to adopt a deformation potential viewpoint. Dexter¹³ extended such a treatment to account for the nonperiodicity of a vibrating lattice. Because of the expansions and

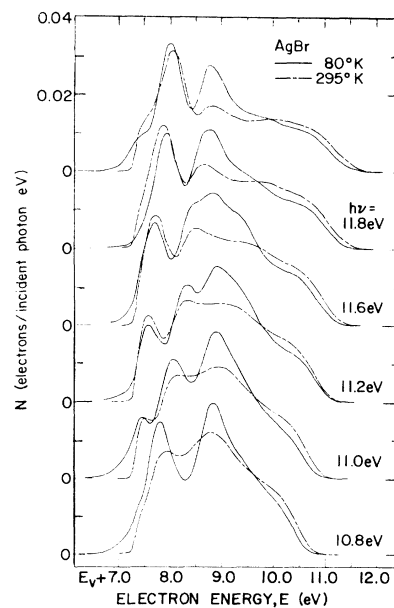


FIG. 2. Comparison of energy distributions normalized to quantum yield (per incident photon) for electrons photoemitted from AgBr at 80 and 295 K for photon energies of 10.8–11.8 eV.

contractions associated with the lattice, there exists local deformation potentials which result in local variations in the band gap. The energy of a state is taken as statistically distributed in accordance with the probability that a constant uniform dilation is realized. This theory employs a simple dilatation for lattice vibrations, thereby completely smoothing phonon details such as dispersion. Local distortion can also be treated in terms of the local vibrations. This approach is based on the usual quadratic Stark shift of the electron energy produced by a uniform electric field¹⁴ or random microfields.¹⁵ Each of these three theories to some degree successfully describes Urbach's rule.¹⁶ Since thermal effects having such an origin must then be significant for too broad a group of solids (e.g., alkali halides, silver halides, amorphous semiconductors) and must describe all electronic states the same, it is clearly not applicable here.

The electronic states must be affected directly by the lattice rather than by an "external" perturbation of the electron's energy. One method of doing this is to explicitly consider the "stationary" (i.e., time-independent), *vibrating*-lattice states of the solid rather than calculating how the states, computed in a periodic nonvibrating frozen lattice, are shifted or broadened due to a departure from periodicity or a change in the lattice constant. This has been attempted in the pseudopotential formalism by using a temperature-dependent form factor obtained for each atomic form factor by multiplying by the Debye-Waller factor.¹⁷ This theory cannot be used directly for our considerations because it only applies to solids which can be treated by pseudopotentials (i.e., where the "weak-binding" approximation is valid). Different considerations are needed for partially ionic solids where the tight-binding approximation works well. By studying this formalism, we are led to describe the thermal effects as a modulation of the near-neighbor wave-function overlap.

B. Dynamic hybridization

Properties of the electronic states in partially ionic A^+B^- solids are most easily understood by a tight-binding description.^{18,19} The energy derived from an atomic orbital n is given by

$$E_{k,n} = \epsilon_n + \frac{(E_n^{(M)} + E_n^{(1)} + E_{k,n}^{(2)})}{1 + S_{k,n}} \quad (1)$$

for the state whose wave function is a linear combination of Bloch sums

$$\Phi_{\vec{k}}(\vec{r}) = \sum_L a_L \sum_j e^{i\vec{k} \cdot \vec{R}_j} \Psi_L(\vec{r} - \vec{R}_j - \delta_L \vec{d}), \quad (2)$$

where \vec{k} is the wave vector, $L \equiv (n, d)$ including

principal and orbital angular momentum quantum numbers, a_L is a normalization factor, $\delta_L = 0$ if Ψ_L 's come from A^+ ions, and $\delta_L = 1$ if Ψ_L 's come from B^- ions. We must then consider the effect of temperature on each of these contributions to the electronic states, viz., ϵ_n is the atomic energy eigenvalue, $E_n^{(M)}$ is the Madelung energy, $E_n^{(1)}$ is a crystal-field correction involving the wave functions on a given site and the potential on a neighboring site, and $E_{k,n}^{(2)}$ and $S_{k,n}$ are the two-center near-neighbor overlap integrals with and without the potential, respectively.

When the interatomic distance is changed due to thermal vibrations and the much smaller accompanying contraction of the lattice, the purely single-center terms ϵ_n are not effected as long as the adiabatic approximation is valid. Of the remaining four terms which all depend on nearest-neighbor distance $|\vec{d}|$, there is an important difference in the overall range of "interaction." The Madelung energy $E^{(M)}$ involves long-range electrostatic potentials from all the ions in the solid, while the "overlapping" terms $E^{(1)}$, $E^{(2)}$, and S are only involved with the short-range potentials and/or wave function located at nearest neighbors. Thus, as $|\vec{d}|$ undergoes random changes due to lattice vibrations, the dynamic variations of near-neighbor contributions will average out when the Madelung sum is taken over many unit cells. The resulting temperature dependence of this energy term can be expected to be many times smaller than those involving overlap. The dynamic ion vibrations *cannot* be properly simulated by a uniform static lattice constant change.²⁰

For partially ionic solids, some near-neighbor terms contribute significantly to the frozen-lattice band structure since wave-function overlap is large and the energy of neighboring A^+B^- states are nearly equal. Further, the wavefunction extent is such that $E^{(2)}$ and S depend strongly on ionic separation. Thus, as the atoms vibrate about their equilibrium lattice position, the dynamic changes in atomic separation caused by the optic modes will produce considerable modulation of the hybridized states. At any instant of time, we optically probe the solid and sample these non-stationary states (i.e., those that change with time). Since the measurement averages over an appropriately long period of time by counting a large number of optical excitations, a broadened level is detected. Such broadening will, of course, be temperature dependent, for as the temperature is lowered, the dynamical motion of the lattice is significantly reduced. This will result in smaller fluctuations of the hybridization with a corresponding reduction in broadening. Since the wave-function hybridization is affected by the dynamic mo-

tion of the lattice, we refer to this effect as “dynamic hybridization.” The shifts caused by the contraction of the lattice upon cooling are negligible compared to this effect. Since it depends critically on the nature of the atomic orbitals, this process is material and electronic state specific, as required by experiment. This last property allows it to be used for identifying the atomic origin of certain regions of the density of states.

Not only will the energy of the state exhibit dynamic hybridization, but also the wave function corresponding to E will change. This is a direct result of thermal modulation in the hybridization coefficients a_L , which enter the Bloch sums formed from different ionic orbitals [see Eq. (2)]. Thus, optical transition matrix elements will depend on temperature and will “project” the temperature-dependent density of states differently for different $h\nu$ and final states.¹² However, this effect alone does not explain the dependence of the data on material.

The electronic state broadening we discuss is many times greater than the thermal energy $k_B T$. There may be some question as to how this can occur, since the maximum energy which can be transferred to the electronic states is only the energy in the vibrating lattice. The important point is that this is true for *all* the states in the solid taken together. When a p -derived state is increased in energy due to the atomic motion, the net energy of the d -derived states with which it mixes will decrease by nearly the same amount. Thus, the individual hybridized states may be shifted by a much greater amount than $k_B T$. This occurrence for the hybridization of electronic states is equivalent to the more familiar crystal-field-splitting case where the average energy of the split levels is always equal to the energy of the unperturbed state (taking degeneracy into account).

It is important to realize that this process limits the range of validity of the Born-Oppenheimer approximation.²¹ Since the lattice vibrations directly affect the electronic states, wave functions of the hybridized states of partially ionic solids cannot be separated into an electronic and a nuclear part. This implies that one cannot consider separate electron and phonon states, and that the electron-lattice interaction cannot be treated by perturbation theory.

IV. MODEL CALCULATIONS

The dynamic hybridization description satisfies the general features of experiment presented in Figs. 1 and 2. To show that it is physically reasonable, we must make quantitative arguments

which at least yield the proper order of magnitudes for the experimental peak broadening and its temperature dependence. We assume constant matrix elements, thereby computing thermal modulation effects on the density of states alone. The silver halides are taken as exemplary partially ionic materials, and their valence states involve orbital mixing typical of some conduction states in ionic compounds. Because of the similarity between AgCl and AgBr properties, we can apply the general conclusions determined for one compound to both when only limited information is available.

A. Lattice vibrations

We must first accurately describe the thermal vibrations of the lattice. Probably the most convenient temperature parameter describing the dynamical motion of the lattice is the Debye temperature Θ_D . This normally corresponds to the temperature at which optic phonons are first excited. The rms displacement of the atoms as a function of temperature can be calculated using the Debye-Waller theory.²² The mean-square amplitude of vibration of each atom in a monatomic solid, with one atom per unit cell of mass m , is given by

$$u^2 = \frac{9\hbar^2 T^2}{mk_B \Theta_D} \left[\left(\frac{\Theta_D}{2T} \right)^2 + \int_0^{\Theta_D/T} \frac{\chi}{e^\chi - 1} d\chi \right]. \quad (3)$$

A good first approximation to the calculation of the vibrations of each ion of a diatomic solid is to assume an equal displacement for the two types of ions, each one having a mass which is the mean of the two constituents \bar{m} .²³ The resulting temperature dependence is shown for AgCl in Fig. 3 for $\bar{m} = 71.7$ amu and $\Theta_D = 162^\circ\text{K}$. The contraction of the lattice constant a upon cooling from room temperature to 80°K is shown for comparison to the vibrational amplitudes.²⁴ The rms displacements for each ion, as determined from neutron-diffraction measurements,²⁵ are surprisingly close, being within 10% and showing the same functional behavior. The interesting conclusion that can be drawn from these results alone is that the amplitudes of vibration for partially ionic solids are typical of most materials and are thus *not* a characteristic feature of dynamic hybridization effects.

B. Electronic states

The valence states of AgCl were calculated using the tight-binding approximation discussed above. The tight-binding matrix elements were obtained using the Slater-Koster method.²⁶ For the cubic (NaCl) structure O_h^2 , elements along the line $\Gamma \rightarrow \Lambda \rightarrow L$ for first and second nearest neighbors, in

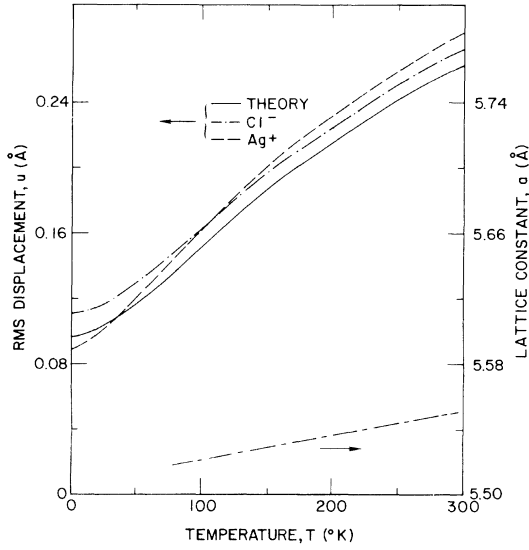


FIG. 3. Temperature dependence of the AgCl rms displacement calculated using Eq. (3) and measured by Vijayaraghavan *et al.* (Ref. 25). The contraction of the lattice from 295 to 80 °K (Ref. 24) is included for comparison.

the two-center approximation, are given in Table I. The secular equation is then a 9×9 determinant whose basis functions are the one Cl $3s$ orbital (s), three Cl $3p$ states (x, y, z), and the first Ag $4d$ states ($xy, yz, zx, x^2 - y^2, 3z^2 - r^2$). The numerical values used for the parameters in the matrix elements (e.g., $pd\sigma$) were those determined by Bassani, Knox, and Fowler for the assumption that only the nearest-neighbor interactions were important.²⁷ Since our interest here is in determining the importance of the various contributions to the energy in Eq. (1) and in particular the effect of the wave-function hybridization on the states, calculations of the energies at Γ and L alone are sufficient. Diagonalizing this secular equation, the resulting magnitudes of each of the contributions to the energy are shown in Fig. 4.

When wave-function normalization is taken into account in Fig. 4(c), the d -derived states at Γ are higher in energy than the p -derived Γ orbitals. It is interesting to note that this contribution which involves overlap between the wave functions of the two atomic species causes the order of the levels to reverse at Γ and produces the large separation

TABLE I. Hamiltonian tight-binding matrix elements for the cubic (NaCl) lattice O_h^5 , along the line $\Gamma \rightarrow \Lambda \rightarrow L$ for first, 1, and second, 2, neighbors in the two-center approximation.^a

(s/s)	$12(ss\sigma)_1 \cos^2\xi + 6(ss\sigma)_2 \cos 2\xi$
(s/x)	$[2\sqrt{2}i(sp\sigma)_1 + 2i(sp\sigma)_2] \sin 2\xi$
(s/xy)	$-2\sqrt{3}(sp\sigma)_1 \sin^2\xi$
$(x/x), (y/y), (z/z)$	$[4(pp\sigma)_1 + 8(pp\sigma)_2] \cos^2\xi + [2(pp\sigma)_2 + 4(pp\sigma)_1] \cos 2\xi$
(x/y)	$[2(pp\pi)_1 - 2(pp\pi)_2] \sin^2\xi$
(x/xy)	$[\frac{1}{2}\sqrt{6}i(pd\sigma)_1 + \sqrt{2}i(pd\pi)_1 + 2i(pd\pi)_2] \sin 2\xi$
(x/yz)	0
$(x/x^2 - y^2)$	$[(3/\sqrt{2})i(pd\pi)_1 - \frac{1}{2}\sqrt{3}i(pd\sigma)_1 + \sqrt{3}(pd\sigma)_2] \sin 2\xi$
$(x/3z^2 - r^2)$	$[\frac{1}{4}\sqrt{2}i(pd\sigma)_1 - \frac{1}{2}\sqrt{6}i(pd\pi)_1 - i(pd\sigma)_2] \sin 2\xi$
$(z/3z^2 - r^2)$	$[(1/\sqrt{2})i(pd\sigma)_1 + \sqrt{6}i(pd\pi)_1 + 2i(pd\sigma)_2] \sin 2\xi$
(xy/xy)	$[3(dd\sigma)_1 + 4(dd\pi)_1 + 5(dd\delta)_1] \cos^2\xi + [4(dd\pi)_2 + 2(dd\delta)_2] \cos 2\xi$
(xy/xz)	$[2(dd\delta)_1 - 2(dd\pi)_1] \sin^2\xi$
$(xy/x^2 - y^2)$	0
$(xy/3z^2 - r^2)$	$[\sqrt{3}(dd\sigma)_1 - \sqrt{3}(dd\delta)_1] \sin^2\xi$
$(xz/x^2 - y^2)$	$[\frac{3}{2}(dd\delta)_1 - \frac{3}{2}(dd\sigma)_1] \sin^2\xi$
$(xz/3z^2 - r^2)$	$[\frac{1}{2}\sqrt{3}(dd\delta)_1 - \frac{1}{2}\sqrt{3}(dd\sigma)_1] \sin^2\xi$
$(x^2 - y^2/x^2 - y^2), (3z^2 - r^2/3z^2 - r^2)$	$[6(dd\pi)_1 + \frac{3}{2}(dd\sigma)_1 + \frac{9}{2}(dd\delta)_1] \cos^2\xi + [3(dd\sigma)_2 + 3(dd\delta)_2] \cos 2\xi$
$(x^2 - y^2/3z^2 - r^2)$	0

^a $\xi = k_x a = k_y a = k_z a \begin{cases} = 0 \text{ at } \Gamma, \\ = \frac{1}{2}\pi \text{ at } L. \end{cases}$

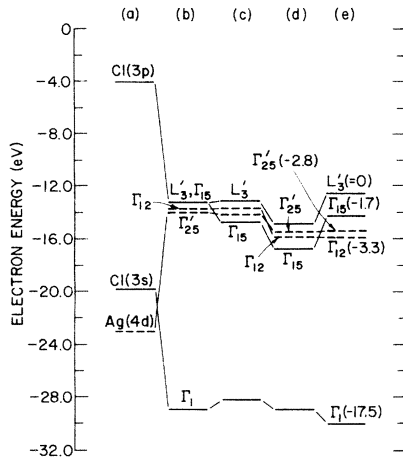


FIG. 4. Contributions to the valence-band structure of AgCl at Γ and the highest valence state at L calculated by the tight-binding approximation Eq. (1): (a) the free ion energy ϵ_n ; to which we add (b) the Madlung energy $E_n^{(M)}$; (c) the wave-function normalization correction $S_{k,n}$ is accounted for; followed by the turning on of (d) the crystal field $E_n^{(1)}$ of the neighbors; and finally (e) the two-center wave-function overlap $E_{k,n}^{(2)}$ is included. The energies of the states, referred to the valence band maximum, are shown in parentheses in part (e).

between the energies of the p -derived state at Γ (Γ_{15}) and the highest L point (L'_3). The crystal-field contribution in Fig. 4(d) simply shifts all the states by roughly the same amount without producing any sizable changes in their relative positions. The two-center overlap term, which is turned on in Fig. 4(e), shifts the p -derived states relative to the d -derived ones thereby producing the ordering of the bands which we deduce from photoemission. It is quite significant that the overlap terms which depend on the p - d mixing have such profound influences on the energy states of the silver halides; it is these same terms which are expected to be the most dependent on temperature due to dynamic motion of the lattice.

C. Dynamic hybridization

Let us then consider the dynamic modulation of electron states in terms of changes in the tight-binding overlap terms. The interaction will be restricted to about one nearest neighbor distance and possible averaging effects are taken to be negligible. Further, only the effect of $k=0$ optical phonons will be considered.

Consider the product of the potential with the normalized free atomic wave functions Ψ_L corresponding to the valence p and d states for nearest neighbors; these orbitals are the actual tight-binding orbitals for the states at Γ [see Eq. (2)]. This term is shown in Fig. 2 of Ref. 6 for the Br

($4p^5$) and Ag ($4d^{10}$) orbitals and atomic potentials from the Herman-Skillman tables.²⁸ In the adiabatic approximation, we can displace the halogen relative to the nearest-neighbor Ag by the rms displacement and recompute the overlap term; the energy contribution is simply the integral of this term. In this manner we estimate that the overlap energy at Γ changes by a third in both AgBr and AgCl due to an optic-mode vibration equal to the rms ionic displacement at room temperature; the normalization term which does not involve the atomic potential changes by over 25%. This crude estimate is within a factor of 2 of a more exact calculation for the $pd\sigma$ overlap in AgCl by Hayns and Calais.²⁹ Since the overlap terms contribute some 2–3 eV to the electronic states, these thermal changes are quite significant (~ 1 eV) and comparable to experimentally observed broadenings.

To obtain more than just this rough illustration of the energy broadening process, we combine the model calculations for the lattice vibrations and the electronic states presented above. To simulate dynamic effects of the ions by computing static changes, we consider variations only in those contributions which depend almost entirely on short-range, primarily nearest-neighbor, interactions; since the atomic motion is random, changes in long-range terms, which involve sums over many unit cells, tend to average out. The two-center overlap term and wave-function normalization are taken as the only contributions which are sensitive to thermal modulation. The ionic displacement influence on the electron energy is simulated by the influence of a contraction or expansion of the lattice on these two p - d mixing terms. We use a very conservative estimate for the lattice constant change which would be reasonably equivalent to the ion motion. If one considers the motion of only one ion in an otherwise frozen lattice, its displacement is also the change in separation between two nearest neighbors (really half the actual rms spacing change). Taking this view, the single ionic displacement is equivalent to the lattice constant change for its particular unit cell edge. Thus, we took the most conservative estimate of allowing the lattice constant to increase and decrease from its equilibrium value by the rms value of the mean ionic displacement (e.g., the room-temperature AgCl lattice dilation is only 0.49 bohr).

We then estimate the thermal broadening by computing the short-range energies for both positive and negative displacement of the ions from equilibrium. From calculations made with an unscreened Slater exchange potential in the course of the work of Ref. 27, Fowler estimates that each of the AgCl two-center integrals (e.g., $pd\sigma$

in Table I) changes by an average of about 5% upon a 1% change in lattice constant.³⁰ We thereby find that the AgCl L'_3 valence-band maximum broadens with temperature in the manner shown in Fig. 5. Though this p -derived state is not directly related to any measured EDC structure, its energy provides an order of magnitude estimate for the experimental broadenings since its large hybridization (i.e., 30% d character²⁷) makes it particularly sensitive to ionic separation. The absolute error in these calculations can be estimated by assuming that the effects of the lattice vibration are "frozen out" at very low temperatures. We then over "correct" the results in Fig. 5 by the using of the zero-point rms displacement (i.e., an AgCl L'_3 broadening of 0.3 eV at 0°K).

The theoretical results are compared with experiment in Table II. On the right-hand side of Table II, calculations to determine the effect of the lattice contraction are presented. As can be seen, the contraction produces shifts of less than 0.1 eV upon cooling from 295 to 80°K and, of course, no change in broadening. Our simple calculation thus indicates that the lattice vibrational modulation of the overlap produces fluctuations in the energies of the hybridized states which are the same magnitude as the observed broadening of photoemission EDC's. These rough calculations further indicate that the changes of these energy variations upon temperature reduction are of the same order of magnitude as the measured EDC temperature dependences. In addition, since the broadening depends on the amplitude of the ionic vibration, the gradual dependence on temperature seen in our experiments

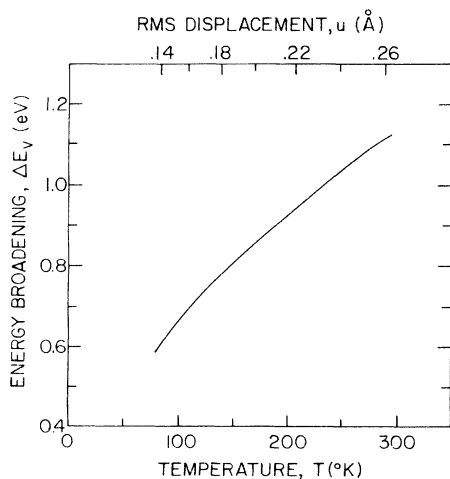


FIG. 5. Temperature and lattice-vibration-amplitude dependence of the broadening of the AgCl valence-band maximum L'_3 .

TABLE II. Comparison of the temperature dependences of the 90% EDC widths of AgCl (AgBr) and the computed broadening of the valence-band maximum (ΔE_v) of AgCl. The calculations used the tight-binding bands for both the rms displacement (u) and the contraction of the lattice (Δa) upon cooling from room to liquid-nitrogen temperature.

T (°K)	90% EDC width ^b (eV)	u (Å)	ΔE_v (eV)	a^a (Å)	ΔE_v (eV)
295	0.5(0.6)	0.26	0.8	5.550	0
80	0.3(0.3)	0.14	0.3	5.517	<0.1
295→80	0.2(0.3)	0.12	0.5	0.033	<0.1

^a Reference 24.

^b AgCl (AgBr), $h\nu = 11.6$ (10.2) eV.

is to be expected. It is further evident that an EDC peak can exhibit a large broadening $> 10k_B\Delta T$ yet a minor energy shift $\sim k_B\Delta T$. We believe that the success of our conservative simulation of dynamic effects in terms of purely hybridization variations is persuasive evidence for the new electron-lattice interaction reported in this paper.

V. DISCUSSION

A. Partially ionic solids

The strong electron-lattice interaction is observed in a very limited number of solids. The conditions which have to be met for a material to possess this property can be stated as follows. (i) Electronic wave functions have to be localized on individual atomic sites enough for the tight-binding approximation to be a good description of the electronic structure. This eliminates solids such as metals or predominantly covalent crystals whose electronic wave functions are so extended that random variations in $|\vec{d}|$ hardly modulate $E^{(2)}$ or S in Eq. (1). (ii) The electronic wave function should not be localized to the point where the amplitude change of lattice vibration hardly modulates the orbital overlap between two nearest-neighbor ions. (iii) The Ψ_L must be atomic species which are compatible for mixing. Further, their energies (i.e., $\epsilon_n + E^{(M)}$) must be reasonably close to each other for the wave-function $\Phi_{\vec{k}}$ to contain a considerable amount of hybridization between the two Bloch sums. (iv) The range of temperature variation should contain or be near Θ_D in order to change the amplitude of lattice vibration significantly.

Each of the four materials in Figs. 1(a)–1(d) does not exhibit dynamic hybridization effects in the temperature-variable EDC's because they fail to satisfy one of these criteria. Ge fails to meet the first condition, the molecular crystal metal-free phthalocyanine fails to meet the second re-

quirement, the valence states of CsI (and LiI)³ the third, and the transition metal oxide V_4O_8 the fourth since $\Theta_D = 750$ °K. On the other hand, TiCl, CuBr, and AgBr exhibit EDC changes which are many times $k_B \Delta T$ because each one satisfies all four conditions.⁴⁻⁶ All materials are ionic with considerable amount of covalent binding; this makes the electronic wave function somewhat extended yet localized enough to be treated in the tight-binding approximation. The ionic energy levels of the halogen outer p orbitals are fairly close to those of the metal s (in Tl^+) or d orbitals (in Cu^+ or Ag^+); thus, the valence electronic states are expected to be hybridizations between the halogen and metal orbitals. The Debye temperatures of 140 °K, 164–222 °K, and 144 °K for the TiCl, CuBr, and AgBr, respectively, are well within the range of experimental temperature variation between 77 and 295 °K; the lattice vibration amplitudes then increase by more than 90% over this temperature range.

The number of substances which have filled electronic states satisfying these criteria are few. Ionicity provides at least an indirect measure of the first two requirements if one limits consideration to valence states exhibiting dynamic hybridization. Using our experience, one would expect materials with ionicity between that of AgCl and CuBr to be prime candidates. These compounds define a narrow range about the critical Phillips–Van Vechten value¹ as shown in Fig. 6. It is solids which have ionicity roughly in this range ($0.86 > f_i > 0.73$) that we term partially ionic. Both AgBr and AgI have intermediate ionicities and do exhibit some EDC structure with an anomalously large temperature dependence.² We may then predict on the basis of Fig. 6 that the following materials may exhibit properties related to a strong valence-electron–lattice interaction: MgO, MgS, MgSe, CuF, CuCl, CdO, CdS, CdSe, and CdTe.

B. Electronic states

The basic microscopic mechanism discussed in this paper is very general and need not be limited simply to valence electrons. When valence wave functions are strongly localized and a large ionicity results (e.g., in alkali halides), some higher energy conduction state orbitals should have the proper characteristics for a large dynamic hybridization energy component. There is evidence for this in the high-energy EDC's of CsI [Fig. 1(h)] and the temperature-dependent optical spectra of alkali halides.³¹ For example, in Fig. 15 of Ref. 31 the A_1-A_2 lines of KBr at $h\nu = 19.8$ eV show many tenths of an eV broaden-

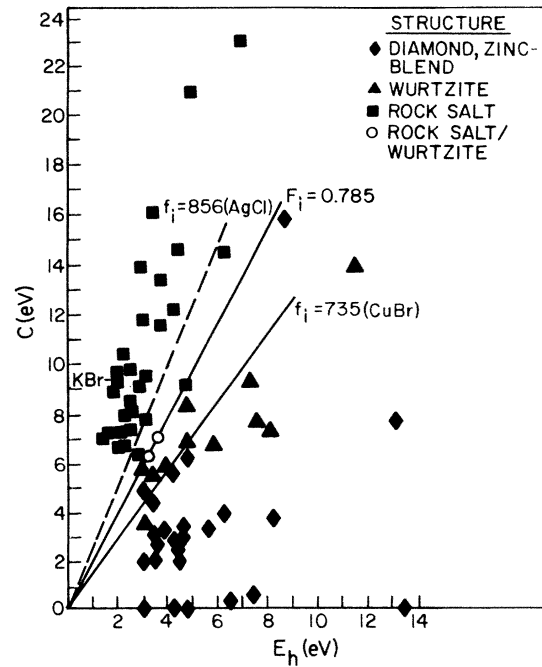


FIG. 6. Separation of fourfold and sixfold coordinated structures into ionic ($f_i > 0.86$), partially ionic or partially covalent ($0.86 > f_i > 0.73$), and covalent ($f_i < 0.73$) crystals. The C -vs- E_h plot of compounds is from Ref. 1.

ing at room temperature.

From such temperature-dependent photoemission and optical data, the atomic origin of density-of-states structure can often be deduced. This is based on the result that only the hybridized electronic states strongly interact with the lattice. Thus, from Fig. 1(g) the upper filled states of AgBr are formed from hybridized mixtures of Br ($4p$) and Ag ($4d$) orbitals. From the band calculations in Fig. 4(e),²⁷ these states are clearly derived from the halogen p levels. Similarly, we propose that the 19.8-eV A_1-A_2 structure in KBr reflectance³¹ involves final states which are hybridizations of K ($4p$) and Br ($4d$) orbitals; a study of KBr band-structure calculations³² reveals that this is quite possible. The average of the widely differing Γ_{12} locations places this d level at almost the identical energy as the Γ_{15c} conduction p state. The resulting hybridized state is ~ 19 eV from the valence band consistent with our assignment.

It follows that one may be able to determine the nature of peaks which lie close to highly temperature sensitive structure but do not themselves exhibit excessive thermal broadening. When forming hybridized states, some of the orbitals will not mix due to symmetry incompatibility; these usually originate from the atomic state having higher orbital quantum number. Thus, the temperature-

independent AgBr EDC structure at -3.7 eV in Fig. 2 is identified as originating from Ag states with almost pure $4d$ symmetry (i.e., those d states which do not mix with neighboring Br p electrons). By varying the vibrational energy of the lattice through temperature variation, we have a method of separating out hybridized states from spatially and energetically nearby "purer" electronic levels.⁶

C. Vibrational states

A natural question arises as to whether this electron-lattice interaction has a corresponding influence on the vibrational states. The phonon dispersion curves of CuCl,³³ and AgBr,³⁴ have recently been found to exhibit anomalous characteristics compared with compounds of the same crystal structure in which the d electrons did not contribute to the bonding orbitals. Serious difficulties in attempts to fit the data with usual force constant and/or shell models occur because of important differences for acoustic modes which mix with optic modes (mainly transverse). This is illustrated for the $[110]$ dispersion of CuCl and its isoelectronic counterparts ZnS,³⁵ and GaP,³⁶ in Fig. 7. It has been suggested^{37,38} that the curious shape of CuCl shown in Fig. 7 and resulting theoretical difficulties were due to interactions between $3d$ electrons on second-neighbor Cu ions.

While we agree that the unique phonon properties must correlate with the presence of d electrons in these types of solids, our experience with electronic properties unique to the same class of materials leads us to a different microscopic origin. We propose that these anomalies occur because of a large displacement-dependent *near-neighbor* electronic wave-function hybridization. The lattice vibrations view this displacement-dependent hybridization as a changing potential in which the ion finds itself as it moves away from its equilibrium position in the lattice. This should lead to large *temperature-dependent* contributions to the phonon dispersion. There is recent evidence³⁹ that the low-temperature phonon dispersion of CuCl differs significantly from room-temperature values³³ (Fig. 7). While this process happens to involve d states in noble-metal halides, it should not be limited simply to d -band solids. For example, we would expect TlCl to have unusual vibrational properties because of s - p mixing (see Ref. 4). Further, the materials which Fig. 6 predict will exhibit dynamic valence-state hybridization effects are also candidates for phonon anomalies. Based on the results of Fisher for AgCl,⁴⁰ and the results of Vardeny

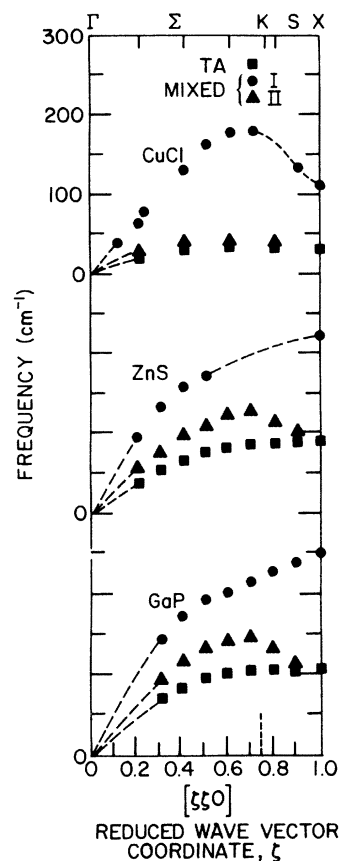


FIG. 7. Dispersion curves for the acoustic modes of CuCl, ZnS, and GaP along the $[110]$ direction at room temperature. The data points and experimental estimates (---) are from Ref. 33, 35, and 36, respectively.

et al. for CuCl,³⁸ these new contributions to the dispersion should be primarily harmonic in character; sophisticated treatments of anharmonic effects are probably not necessary to theoretically model the interaction.

VI. CONCLUSION

The major new feature of this work is the discovery of a temperature dependence of certain structure in the energy distributions of photoemitted electrons which is an order of magnitude greater than the change in thermal energy $k_B T$. This probably represents the first observation of what may prove to be a whole new class of electron-lattice effects in solids which satisfy the general criteria listed in Sec. V A. For example, the properties of superconductors may be affected by the same mechanism. Since this process perturbs the normal electron-lattice interaction so strongly, we expect modifications to the electron-phonon coupling responsible for

superconducting behavior.

This dynamic hybridization process was able to explain the material and electronic state selectivity evident in the photoemission data. By using a very simple approximation of $k=0$ optical phonons and restricting the extent of the interaction to about one nearest neighbor distance, the proper magnitudes for density-of-states peak broadenings and their temperature dependences were calculated. A model-independent application of this mechanism allowed the silver states with almost pure $4d$ symmetry in the silver halides and the hybridizing conduction d states in KBr to be identified directly from experiment.

In order to obtain further information, both the data and physical process must be treated in more detail. For example, we find that the EDC peak width W broadens exponentially with temperature according to

$$W = W_0 \exp[C(T/\Theta_D)]. \quad (4)$$

W_0 measures the EDC width corresponding to zero-point vibrations, while the slope C is a measure of the temperature dependence of the density-of-states broadening. This is illustrated in Fig. 8 for the direct transition peak of AgBr in the $h\nu=10.2$ eV EDC's.

The exponential dependence occurs for peaks in all the silver halides and is relatively insensitive to the photon energy of measurement as shown by Table III. Note that the average parameters for the halogen p -derived structure are nearly identical for AgBr ($W_0=0.29$ eV, $C=0.35$) and AgCl ($W_0=0.27$ eV, $C=0.35$); this common

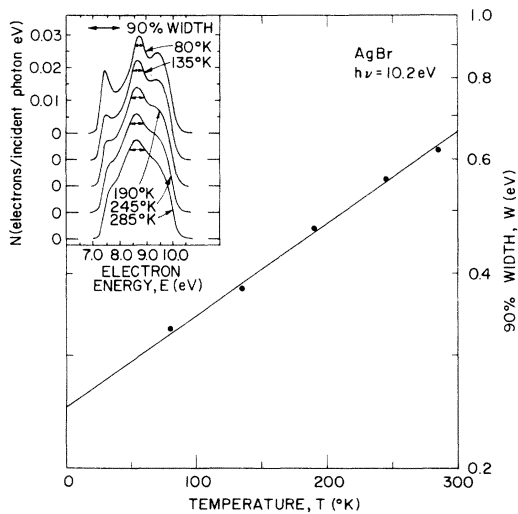


FIG. 8. Temperature dependence of the AgBr, $h\nu=10.2$ eV EDC width measured at 90% of its maximum height, as shown in the insert. The straight line corresponds to the equation $W=0.25 \exp[0.47(T/\Theta_D)]$.

TABLE III. Characteristic parameters defined by Eq. (4) for the exponential temperature dependence of silver-halide EDC peak widths. The width, measured at 90% of maximum peak height, spans the peak unless indicated by l for left or r for right half-width. The peak is identified by its initial- E_i or final- E_f state energy where applicable.

Material	$h\nu$ (eV)	W_0 (eV)	C
AgBr	10.8	0.32	0.33
	10.2	0.25	0.47
	9.7	0.15(l)	0.27
	9.2	0.14(l)	0.32
AgCl ^a	11.8	0.14(r)	0.35
	11.6	0.11(r)	0.47
	11.2	0.13(r)	0.28
	11.0	0.31	0.28
AgI(β)	11.3 ^b	0.47	0.22
	10.6 ^b	0.49	0.17
	9.2 ^c	0.29	0.15
	8.1 ^d	0.14(l)	0.14

^a $E_i = -2.65$ eV.

^b $E_i = -1.17$ eV.

^c $E_f = 7.8$ eV.

^d $E_f \approx 7.1$ eV.

value of $C \approx \frac{1}{3}$ may be a basic constant describing the effect. As ionicity decreases with the increasing covalent bonding of β -AgI, the dynamic effects on hybridization energies decrease (i.e., $C=0.17$).

The many-body nature of the interaction makes the theoretical problem very complex. As in the case of the Jahn-Teller effect, the frozen-lattice approximation is not valid, and one must really consider wave functions of the entire solid (e.g., vibronic states) rather than separate electronic and nuclear parts. The concepts of a frozen-lattice energy band structure and well-defined temperature-independent phonons must be applied with caution. Doniach has used a Green's-function method to account for random variations in tight-binding overlaps induced by the ionic motion.⁴¹ To first order, the temperature dependence of density-of-states structure is found to be the same as the EDC width dependence [i.e., Eq. (4)]. C may be useful as a quantitative measure of the amount of hybridization of the electronic states corresponding to a particular EDC peak, as suggested by the experimental trends. These early theoretical results support the view that the important thermal modulation occurs for the density of electronic states rather than for matrix elements which depend on a particular experimental probe. They further indicate that the dynamic hybridization picture is, in general, a proper representation for the physical phenomenon.

ACKNOWLEDGMENTS

The authors gratefully acknowledge stimulating discussions with J. L. Beeby, A. H. Bienenstock, S. Doniach, W. B. Fowler, and T. H. Geballe.

*All experimental work was done at Stanford University under NASA Contract No. NGR 05-020-066.

- ¹J. C. Phillips and J. A. Van Vechten, *Phys. Rev. Lett.* **22**, 705 (1969); J. A. Van Vechten, *Phys. Rev.* **187**, 1007 (1969); and J. C. Phillips, *Rev. Mod. Phys.* **12**, 317 (1970).
- ²R. S. Bauer and W. E. Spicer, following paper, *Phys. Rev. B* **14**, 4539 (1976); R. S. Bauer, Ph.D. dissertation (Stanford University, 1970) (unpublished) (Xerox University Microfilms No. 71-19646).
- ³R. S. Bauer and W. E. Spicer, *Phys. Rev. Lett.* **25**, 1283 (1970).
- ⁴S. F. Lin and W. E. Spicer, second following paper, *Phys. Rev. B* **14**, 4551 (1976).
- ⁵S. F. Lin, W. E. Spicer, and R. S. Bauer, third following paper, *Phys. Rev. B* **14**, 4559 (1976).
- ⁶R. S. Bauer and W. E. Spicer, *Electron Spectroscopy*, edited by D. A. Shirley (North-Holland, Amsterdam, 1972), p. 569.
- ⁷W. E. Spicer, *Phys. Rev.* **112**, 114 (1958); *Optical Properties of Solids—New Developments*, edited by B. O. Seraphin (North-Holland, Amsterdam, 1976), p. 633-676.
- ⁸K. K. Thornber and R. P. Feynman, *Phys. Rev. B* **1**, 4099 (1970).
- ⁹G. Ascarelli, *Phys. Rev. Lett.* **20**, 44 (1968); *Phys. Lett. A* **26**, 269 (1968).
- ¹⁰R. Stuart, F. Wooten, and W. E. Spicer, *Phys. Rev.* **135**, A495 (1964).
- ¹¹M. G. Mason, *Phys. Rev. B* **11**, 5094 (1975).
- ¹²J. Tejada, N. J. Shevchik, W. Braun, A. Goldman, and M. Cardona, *Phys. Rev. B* **12**, 1557 (1975).
- ¹³D. L. Dexter, *Nuovo Cimento Suppl.* **VII**, No. 2, 245 (1958).
- ¹⁴D. L. Dexter, *Phys. Rev. Lett.* **19**, 1383 (1967); and A. Radowsky, *Phys. Rev.* **73**, 749 (1948).
- ¹⁵J. D. Dow and D. Redfield, *Phys. Rev. Lett.* **26**, 762 (1971).
- ¹⁶F. Urbach, *Phys. Rev.* **92**, 1324 (1953). For a good general review, see R. S. Knox, *Theory of Excitons*, Suppl. 5 to *Solid State Physics*, edited by F. Seitz and D. Turnbull (Academic, New York, 1963), p. 155.
- ¹⁷C. Keffer, T. M. Hayes, and A. Bienenstock, *Phys. Rev. B* **2**, 1966 (1970).
- ¹⁸The complete tight-binding formulation of dynamic hybridization is presented in Ref. 2.
- ¹⁹E. Calabrese and W. B. Fowler, *Phys. Status Solidi B* **56**, 621 (1973); and E. Calabrese, Ph.D. dissertation (Lehigh University, 1970) (unpublished) (Xerox University Microfilms No. 71-17076).
- ²⁰W. B. Fowler, *Phys. Status Solidi B* **52**, 591 (1972). Compare this static simulation of a dynamic band effect to that of J. S. Melvin and T. Smith, *Solid State Commun.* **11**, 1723 (1972).
- ²¹J. C. Slater, *Quantum Theory of Molecules and Solids* (McGraw-Hill, New York, 1963), Vol. 1, p. 9.
- ²²J. M. Ziman, *Principles of the Theory of Solids* (Cambridge U.P., London, 1965), p. 60.
- ²³R. W. James and E. M. Firth, *Proc. R. Soc. Lond. A* **117**, 62 (1927).
- ²⁴B. R. Lawn, *Acta Crystallogr.* **16**, 1163 (1963).
- ²⁵P. R. Vijayaraghavan, R. M. Nicklow, H. G. Smith, and M. K. Wilkinson, *Phys. Rev. B* **1**, 4819 (1970).
- ²⁶J. C. Slater and G. F. Koster, *Phys. Rev.* **94**, 1498 (1954). This paper does not present the matrix elements for the cubic (NaCl) structure given in Table I.
- ²⁷F. Bassani, R. S. Knox, and W. B. Fowler, *Phys. Rev.* **137**, A1217 (1965).
- ²⁸F. Herman and S. Skillman, *Atomic Structure Calculations* (Prentice-Hall, Englewood Cliffs, N. J., 1963).
- ²⁹M. R. Hayns and J. L. Calais, *J. Chem. Phys.* **57**, 147 (1972).
- ³⁰W. B. Fowler (private communication).
- ³¹G. W. Rubloff, *Phys. Rev. B* **5**, 662 (1972).
- ³²A. B. Kunz, *Phys. Status Solidi* **29**, 115 (1968); and L. J. Page and E. H. Hygh, *Phys. Rev. B* **1**, 3472 (1970).
- ³³C. Carabatos, B. Hennion, K. Kunc, F. Moussa, and C. Schwab, *Phys. Rev. Lett.* **26**, 770 (1971).
- ³⁴W. von der Osten and B. Dorner, *Solid State Commun.* **16**, 431 (1975).
- ³⁵L. A. Feldkamp, F. Venkataraman, and J. S. King, *Solid State Commun.* **7**, 1571 (1969).
- ³⁶J. L. Yarnell, J. L. Warren, R. G. Wnezel, and P. J. Dean, Proceedings of the IAAE Symposium on Neutron Inelastic Scattering, Copenhagen, 20-25 May, 1968 (unpublished).
- ³⁷B. Hennion, F. Moussa, B. Prevot, C. Carabatos, and C. Schwab, *Phys. Rev. Lett.* **28**, 964 (1972).
- ³⁸Z. Vardeny, G. Gilat, and A. Pasternak, *Phys. Rev. B* **11**, 5175 (1975).
- ³⁹R. M. Pick (private communication concerning new temperature-dependent neutron diffractions measurements of CuCl by B. Prevot and B. Hennion).
- ⁴⁰K. Fischer, *Phys. Status Solidi B* **66**, 295 (1974).
- ⁴¹S. Doniach (private communication).